JOURNAL OF NANO- AND ELECTRONIC PHYSICS
Vol. **14** No 2, 02025(5pp) (2022)

ЖУРНАЛ НАНО- ТА ЕЛЕКТРОННОЇ ФІЗИКИ
Том **14** № 2, 02025(5cc) (2022)

Characterization of Magnesium/Barium Aluminates Spinel Synthesized by Sol-Gel Auto-Combustion Method

K. Mahi[1,2,*], R. Mostefa[1]

[1] *Department of Physics, Faculty of Matter Sciences, University of Tiaret, BP P 78 Zaaroura, Tiaret, Algeria*
[2] *Laboratory of Plasma Physics, Conductor Materials and their Applications, Faculty of Physics, Oran University of Sciences and Technology Mohamed Boudiaf USTO-MB, BP1505 Oran, Algeria*

(Received 11 March 2022; revised manuscript received 25 April 2022; published online 29 April 2022)

Nanocrystalline magnesium/barium aluminates powder was prepared by a sol-gel auto-combustion method from Al, Mg and Ba nitrates. Mg and Ba elements are among the potential candidates for various applications due to their flexibility, abundance and excellent electromagnetic performance. The phase transformation, crystal structure, functional groups, bonds in the structure and optical properties of the obtained powders were determined by X-ray diffraction, Fourier transform infrared spectroscopy (FTIR) and UV-visible spectroscopy. The electronic band gaps of $MgAl_2O_4$ and $BaAl_2O_4$ calculated using the Tauc method are shown to remain largely unchanged as X (Mg or Ba) is substituted into the lattice, forming XAl_2O_4, but increase greater than 0.05 eV for $MgAl_2O_4$. The X-ray diffraction results reveal that with the X-substitution the crystallite size, cell volume and lattice parameter increase. The incorporation of magnesium and barium atoms into XAl_2O_4 is confirmed by the FTIR spectroscopy. The results show that $MgAl_2O_4$ and $BaAl_2O_4$ spinels can be obtained by sol-gel auto-combustion method at room temperatures (300 K), resulting in a material with high purity and large surface area.

Keywords: Magnesium aluminate, Barium aluminate, Spinel structure, Sol-gel method, Powder synthesis, Nanostructures.

DOI: 10.21272/jnep.14(2).02025 PACS numbers: 81.20.Ka, 81.07.Wx, 81.05.Je

1. INTRODUCTION

Ceramic materials are known for their very interesting physical, chemical and mechanical properties, which differ according to the technique of synthesis and elaboration. The use and application of these materials are extensive such as in mechanical and electronic components, optical magnetic devices, tissue engineering magnetic storage systems and magnetic resonance imaging. Among these materials, aluminates (Al) based spinels with general formula XAl_2O_4 (where X = Mg and Ba) can be considered as a multifunctional material due to its numerous applications, in particular, in the military field: missile domes, transparent armor, thermal camera windows and riflescope. It is also used as catalysts in the environmental field, gas sensors and for energy storage and conversion [1-3]. Moreover, Al-based spinels are stable and environmentally friendly materials.

It has known that the synthesis method can affect the crystallinity, purity, particle size, surface area and morphology of nanoparticle XAl_2O_4, which exert a significant influence on their structural and optical properties [4]. XAl_2O_4 can be prepared by various techniques (sol-gel method, solid-state reactions and hydrothermal method), each of these techniques requires its own specialized equipment. The sol-gel auto combustion method has been demonstrated to produce homogeneous high-purity nanoparticles with rapid heating and short reaction time [5-7]. This synthesis method combines the chemical sol-gel and combustion process, representing a quick, accessible technique with low energy costs and ideal for the synthesis of materials based on metal oxides.

Here, we report the facile synthesis of $MgAl_2O_4$ and $BaAl_2O_4$ spinel-type oxides via simple approach of the sol-gel auto-combustion process. These samples are characterized by Ultraviolet-visible diffuse reflectance spectroscopy (UV-Vis), Fourier Transform Infrared Spectroscopy (FTIR) and Powder X-ray diffraction (XRD) techniques in order to investigate their optical and structural properties. The present work aims to bridge the knowledge gap by utilizing the favorable properties of $MgAl_2O_4$ and $BaAl_2O_4$ samples to produce a potential candidate for various applications, such as catalysts, water treatment and refractory cements.

2. MATERIALS AND METHODS

2.1 Preparation of $MgAl_2O_4$ and $BaAl_2O_4$

$MgAl_2O_4$ and $BaAl_2O_4$ were synthesized by sol-gel auto-combustion method using a mixture of aluminum nitrate nonahydrate (sigma Aldrich, purity 99.99 %) and urea as complexing agent, with magnesium nitrate tetrahydrate (sigma Aldrich, purity 99.00 %), and barium nitrate (sigma Aldrich, purity 99.00 %) as precursors, respectively. All the chemicals were used as such without any further purification. The starting materials were supplied all in analytical pure grade (Merck-Germany). The different initial precursor quantities and chemical formula are shown in Table 1.

The stoichiometric proportions of aluminum nitrate, magnesium nitrate, barium nitrate and urea are dissolved in an amount of distilled water (100 ml). The mixture was heated to 200 °C while stirring constantly.

* khaled.mahi@univ-tiaret.dz
mahikhalidou@yahoo.fr

 © 2022 Sumy State University

After evaporation, the solution converts into wet gel. The gel is then heated at high temperatures in order to get a dry gel. Finally, the as-synthesized powders were calcined in air at 900 °C for 4 h. The sol-gel auto combustion method was used to prepare spinel type oxides (XAl_2O_4, X = Mg, Ba) in several steps, as shown in Fig. 1.

Table 1 – Quantity and chemical formula of the raw materials used to synthesize both structures

Material	Chemical formula	Quantity (g)
Aluminum nitrate	$Al(NO_3)_3 \cdot 9H_2O$	10.0
Magnesium nitrate	$Mg(NO_3)_2 \cdot 4H_2O$	3.15
Barium nitrate	$Ba(NO_3)_2$	3.48
Urea	$CO(NH_2)_2$	5.35

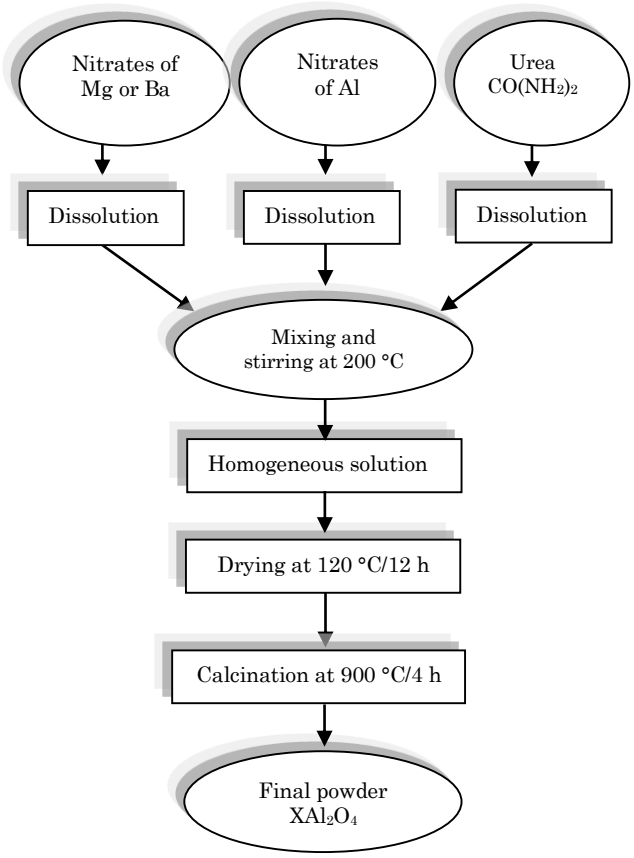

Fig. 1 – The schematic flow chart for the formation of $MgAl_2O_4$ and $BaAl_2O_4$ nanocrystals by sol-gel auto-combustion method

2.2 Characterization Techniques

Crystallographic analysis of the nanoparticles obtained was performed using a PHLIPS PW 1800 powder diffractometer operated at 40 kV and 20 mA with radiation ($\lambda = 1.54$ Å) and scattering angle 2θ ranging from 10° to 90°. Spectroscopic analysis of the samples was carried out using FTIR in KBr pellets in the wavenumber range from 4000 to 400 cm^{-1}. Diffuse reflectance UV-Vis spectroscopy (SHIMADZU UV-1650-PC) in a wavelength range between 200 and 900 nm was used in order to find the optical properties and band gap energy (E_g) of the nanopowders obtained at room temperature.

3. RESULTS AND DISCUSSION

3.1 UV-Visible Analysis

In this part, the UV-Vis spectra of all samples were recorded in the wavelength range from 200 to 900 nm. Fig. 2 represents the UV-Vis transmittance spectra of $MgAl_2O_4$ and $BaAl_2O_4$ powders. Both structures exhibit better transmittance in the visible region of about 97 % indicating good transparency of the studied samples. The absorption spectra of $MgAl_2O_4$ and $BaAl_2O_4$ samples are shown in Fig. 3. We observe that the two structures can efficiently absorb energy below 310 nm, allowing them to be considered UV activated photocatalysts. Additionally, it is possible to observe an absorption peak between 350 and 450 nm for $MgAl_2O_4$ and $BaAl_2O_4$.

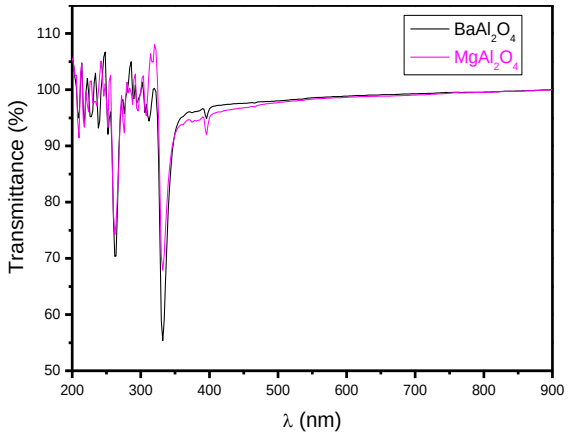

Fig. 2 – UV-Vis transmittance spectra of $MgAl_2O_4$ and $BaAl_2O_4$ powders synthesized by sol-gel auto-combustion method

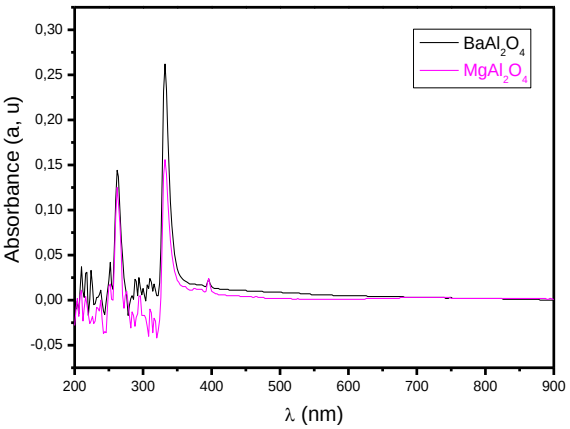

Fig. 3 – UV-Vis absorbance spectra of $MgAl_2O_4$ and $BaAl_2O_4$ powders synthesized by sol-gel auto-combustion method

In order to determine the optical energy band gap of both samples, the UV-Vis absorption spectrum was recorded (Fig. 3). This figure shows a strong absorption peak at 340 nm in the UV region. This can be attributed to photo excitation of electrons from the valence band to the conduction band. The value of the optical energy band gap (E_g) was evaluated by the method proposed by Wood and Tauc, by extrapolating the linear portion of the Tauc's graphs, according to the following equation [8, 9]:

$$(\alpha h\upsilon)^n = A(h\upsilon - E_g),$$

where α is the absorption coefficient, $h\upsilon$ is the light energy, A is a constant, E_g is the band gap energy and n is a constant associated with different types of electronic transitions (n = 1/2, 2, 3/2 and 3 for direct allowed, indirect allowed, direct forbidden and indirect forbidden transitions, respectively).

The plots of quantity $(ahv)^2$ against hv for $MgAl_2O_4$ and $BaAl_2O_4$ samples are represented in Fig. 4 and Fig. 5, respectively. From these curves, the point of intersection of the y-axis with the linear part gives an average value of the band gap equal to 3.676 eV for $MgAl_2O_4$ and 3.626 eV for $BaAl_2O_4$. From the above results, it can be noted that the change of X element caused the reduction in the band gap for magnesium (Mg) cation compared to barium (Ba) cation. A similar observation was noted by C. Gómez-Solís et. al [10].

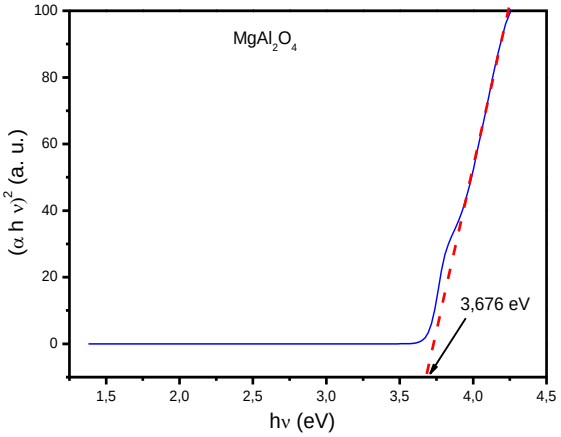

Fig. 4 – Plot of $(ahv)^2$ against photon energy (hv) of $MgAl_2O_4$ powder synthesized by sol-gel auto-combustion method

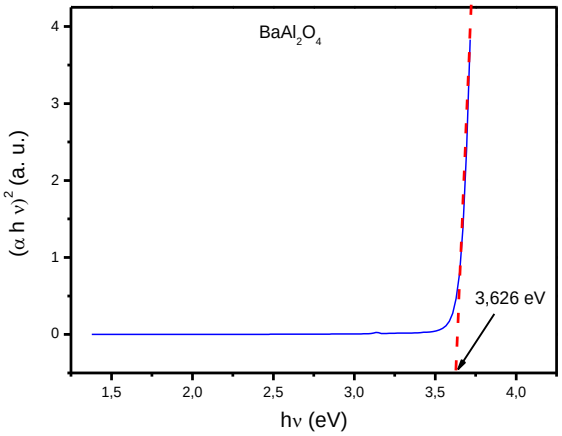

Fig. 5 – Plot of $(ahv)^2$ against photon energy (hv) of $BaAl_2O_4$ powder synthesized by sol-gel auto-combustion method

3.2 X-ray Diffraction Analysis

XRD was used to identify the crystal structure and phase evolution of powders prepared after calcination. According to this method, diffraction patterns are generated from a powdered sample of crystals and compared with reference cards within a database that contains diffraction patterns of known crystals.

Fig. 2 and Fig. 3 show the XRD patterns of $MgAl_2O_4$ and $BaAl_2O_4$ structures synthesized by sol-gel auto-combustion method, respectively. All observed peaks for both structures ($MgAl_2O_4$ and $BaAl_2O_4$) match excellently with ICSD (Inorganic Crystal Structure Data base), data file No. 9010350 and 1010630, respectively. This result indicates the high-purity and crystallinity of these sample synthesized in this work.

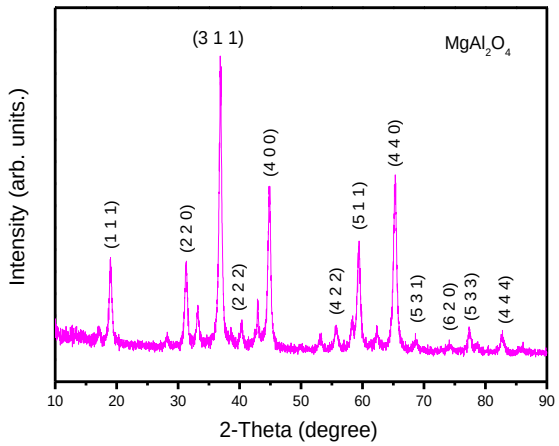

Fig. 6 – X-ray patterns of $MgAl_2O_4$ nanoparticles synthesized by sol-gel auto-combustion method

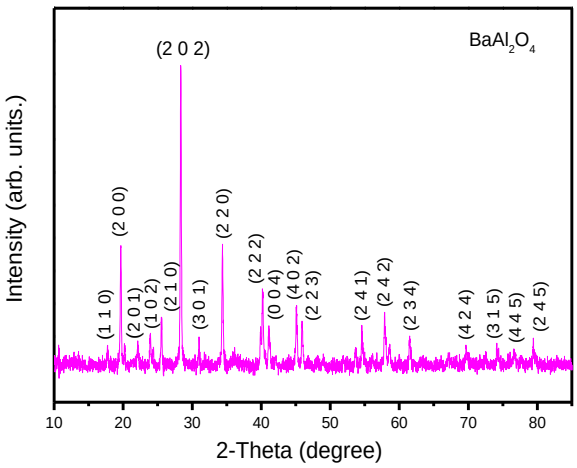

Fig. 7 – X-ray patterns of $BaAl_2O_4$ nanoparticles synthesized by sol-gel auto-combustion method

From the XRD measurement data, we can calculate the crystallite size, lattice constant, and cell volume. The lattice parameters of the prepared samples were estimated from 2θ values of the most intense peak using the Bragg diffraction condition given by [11, 12]:

$$a = \frac{\lambda}{2}\frac{(h^2 + k^2 + l^2)}{\sin\theta},$$

where λ is the wavelength of the X-ray radiation, (hkl) signify the Miller indices, and θ is the diffraction angle corresponding to the most intense reflection plane.

The unit volume (V) of the prepared aluminate spinels was calculated using the expression [13, 14]:

$$V = \frac{\sqrt{3}}{2}a^2 c.$$

The crystallite size is calculated from the full width at half maximum (FWHM (β)) of the diffraction peaks using the Debye-Scherrer method [15, 16] according to the following equation:

$$D = \frac{k\lambda}{\beta \cos\theta},$$

where k is the crystallite shape factor ($k = 089$), λ is the X-ray wavelength ($\lambda = 1.5406$ Å), β is the FWHM, θ is the maximum of the Bragg diffraction peak (in radians), and D is the crystallite size estimated. The results obtained for the lattice parameter (a), crystallite size (D) and cell volume (V) for both samples are summarized in Table 2.

Table 2 – Values of the lattice constant, unit cell volume and average crystalline size calculated from XRD analysis for both samples ($MgAl_2O_4$ and $BaAl_2O_4$)

Parameters calculated	Samples	
	$MgAl_2O_4$	$BaAl_2O_4$
a (Å)	08.08	10.42
b (Å)	08.08	10.42
c (Å)	08.08	08.78
V (Å^3)	527.53	825.58
D (nm)	20.07	34.66

3.3 Fourier Transform Infrared Data Analysis

FTIR analysis was performed to investigate the formation of the metal aluminate spinel structure and surface functional group. The study of atomic and molecular vibrations with the identification of local chemical bonds is possible with the aid of the peaks created in different regions of the IR spectra.

FTIR spectra of $MgAl_2O_4$ and $BaAl_2O_4$ were analyzed as represented in Fig. 8. Vibrations of the bonds in the region 400-600 cm^{-1} correspond to metal ions. The peaks present in this range are due to the presence of divalent metal cations (Mg–O and Ba–O) [17, 18].

$MgAl_2O_4$ and $BaAl_2O_4$ powders exhibit additional minor transmittance bands at 2877, 2455 and 2363vcm^{-1}. Transmittance bands shown by both powders at 3475 and 1746 cm^{-1} correspond to broad –OH stretching and H–O–H bending vibrations, respectively [19]. Additionally, the intense band at 1427 cm^{-1} confirms the asymmetric stretching of tetrahedral AlO_4, indicating the formation of the $MgAl_2O_4$ and $BaAl_2O_4$ phase. This result is consistent with other works, in which powders were synthesized by solution combustion synthesis method similar to that studied in this work.

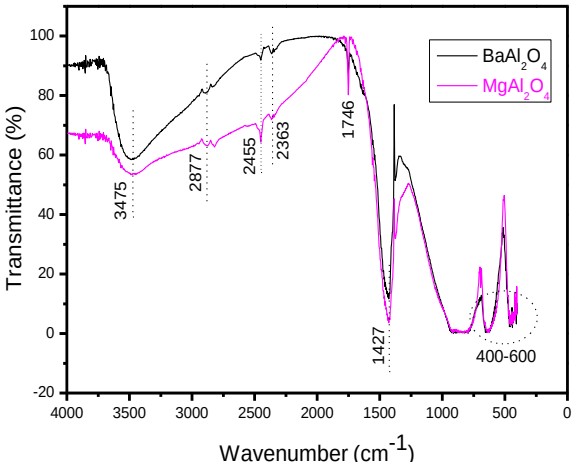

Fig. 8 – FTIR spectra of $MgAl_2O_4$ and $BaAl_2O_4$ powders synthesized by sol-gel auto-combustion method

4. CONCLUSIONS

$MgAl_2O_4$ and $BaAl_2O_4$ nanopowders were prepared successfully using sol-gel auto-combustion method. This method results in materials with important properties for numerous applications. The variation of band gap values can be attributed to structural disorder in the structure, which may change the present energy levels within the band gap. Therefore, the value of E_g may depend on the type of cations present in the spinel structure and synthesis conditions. The XRD results prove the spinel phase for all samples with no secondary phase. The characteristic IR absorption bands in the frequency range of 400-800 cm^{-1} exhibited the expected main absorption bands, thereby confirming the spinel structure. The structural properties of spinel-type aluminates depend upon the method of preparation and the nature of the substituting element.

REFERENCES

1. M.Y. Nassar, I.S. Ahmed, I. Samir, *Spectrochim. Acta A Mol. Biomol. Spectrosc.* **131**, 329 (2014).
2. Y. Uchimoto, K. Amezawa, T. Furushita, M. Wakihara, I. Taniguchi, *Solid State Ionics* **176**, 2377 (2005).
3. M.R. Quirino, M.J.C. Oliveira, D. Keyson, G.L. Lucena, *Mater. Res. Bull.* **74**, 124 (2016).
4. F.M. Stringhini, E.L. Foletto, D. Sallet, *J. Alloy. Compd.* **588**, 305 (2014).
5. S. Kanagesan, M. Hashim, S. Tamilselvan, N.B. Alitheen, I. Ismail, *Dig. J. Nanomater. Biostruct.* **8**, 1601 (2013).
6. C. Ragupathi, J.J. Vijaya, L.J. Kennedy, *Mater. Sci. Eng. B* **184**, 18 (2014).
7. I. Version, A. Gaffoor, D. Ravinder, *Int. J. Eng. Res. Appl.* **4**, 73 (2014).
8. A. Kadari, A. Azaiz, N. Mokhtari D. Horri, *J. Nano- Electron. Phys.* **12** No 6, 06009 (2020).
9. D. Fadil, R.R.F. Hossain, G.A. Saenz, A.P. Kaul, *J. Mater. Chem. C* **5**, 5323 (2017).
10. C. Gómez-Solís, S.L. Peralta-Arriaga, L.M. Torres-Martínez, I. Juárez-Ramírez, L.A. Díaz-Torres, *Fuel* **188**, 197 (2017).
11. R. Tiwari, M. De, H.S. Tewari, S.K. Ghoshal, *Res. Phys.* **16**, 102916 (2020).
12. S.Y. Mulushoa, M.T. Wegayehu, G.T. Aregai, N. Murali, M.S. Reddi, B. Vikram Babu, T. Arunamani, K. Samatha, *Chem. Sci. Trans.* **6**, 653 (2017).
13. K. Mahi, R. Mostefa, *J. Phys. Sci.* **32**, 61 (2021).
14. S. Sahu, P.K. Samanta, *J. Nano- Electron. Phys.* **13** No 5, 05001 (2021).
15. A. Selmi, O. Marwène, H. EL-Kèbir, *J. Molec. Struct.* **1235**, 130262 (2021).
16. B.M. Pradeep Kumar, K.H. Shivaprasad, R.S. Raveendra, R. Hari Krishna, B.M. Nagabhushana, *J. Mater. Sci. Surf.*

Eng. **4**, 923 (2016).
17. T.H. Dolla, K. Pruessner, D.G. Billing, *J. Alloy. Compd.* **742**, 78 (2018).
18. M.Z. Pedram, M. Omidkhah, A.E. Amooghin, *J. Ind. Eng. Chem.* **20**, 74 (2014).
19. I. Ganesh, *Int. Mater. Rev.* **58**, 63 (2013).

Характеристика шпинелі алюмінатів магнію/барію, синтезованих золь-гель методом автогоріння

K. Mahi[1,2], R. Mostefa[1]

[1] *Department of Physics, Faculty of Matter Sciences, University of Tiaret, BP P 78 Zaaroura, Tiaret, Algeria*
[2] *Laboratory of Plasma Physics, Conductor Materials and their Applications, Faculty of Physics, Oran University of Sciences and Technology Mohamed Boudiaf USTO-MB, BP1505 Oran, Algeria*

Нанокристалічний порошок алюмінатів магнію/барію готували золь-гель методом автогоріння з нітратів Al, Mg та Ba. Елементи Mg і Ba є потенційними кандидатами для різних застосувань завдяки їх гнучкості, великої кількості у природі та чудовим електромагнітним характеристикам. Фазові перетворення, кристалічну структуру, функціональні групи, зв'язки в структурі та оптичні властивості отриманих порошків визначали за допомогою рентгенівської дифракції, інфрачервоної спектроскопії з перетворенням Фур'є (FTIR) та УФ-видимої спектроскопії. Показано, що електронні ширини забороненої зони $MgAl_2O_4$ і $BaAl_2O_4$, розраховані за допомогою методу Тауца, залишаються в основному незмінними, оскільки X (Mg або Ba) впроваджуються в решітку, утворюючи XAl_2O_4, але збільшуються більше ніж на 0,05 еВ для $MgAl_2O_4$. Результати рентгенівської дифракції показують, що при X-заміщенні збільшуються розмір кристалітів, об'єм комірки та параметр решітки. Включення атомів магнію та барію в XAl_2O_4 підтверджено спектроскопією FTIR. Результати показують, що шпінелі $MgAl_2O_4$ і $BaAl_2O_4$ можна отримати золь-гель методом автогоріння при кімнатній температурі (300 К), що призводить до отримання матеріалу високої чистоти та великої площі поверхні.

Ключові слова: Алюмінат магнію, Алюмінат барію, Структура шпінелі, Золь-гель метод, Порошковий синтез, Наноструктури.